Journal of Luminescence 131 (2011) 347–351

Contents lists available at ScienceDirect

Journal of Luminescence

journal homepage: www.elsevier.com/locate/jlumin

Ultraviolet emissions from Gd^{3+} ions excited by energy transfer from Ho^{3+} ions

Ying Yu [a], Yangdong Zheng [a], Zhemin Cheng [a], Dan Wang [a], Lixin Liu [a], Feng Qin [a], Changbin Zheng [a], Zhiguo Zhang [a,*], Wenwu Cao [a,b,*]

[a] Department of Physics, Harbin Institute of Technology, Harbin 150001, People's Republic of China
[b] Materials Research Institute, The Pennsylvania State University, University Park, PA 16802, USA

ARTICLE INFO

Article history:
Received 9 June 2010
Received in revised form
7 October 2010
Accepted 28 October 2010
Available online 4 November 2010

Keywords:
Ultraviolet emission
Upconversion
Energy transfer

ABSTRACT

Ultraviolet (UV) upconversion (UC) emissions of Gd^{3+} ion were investigated in $Y_{1.838-x}Gd_xYb_{0.16}Ho_{0.002}O_3$ ($x=0$, 0.16, 0.4, 1, 1.4) bulk ceramics under 976 nm laser diode (LD) excitation. The UC emissions centered at 309 and 315 nm are assigned to the transition of $^6P_{5/2}\rightarrow{}^8S_{7/2}$ (Gd) and $^6P_{7/2}\rightarrow{}^8S_{7/2}$ (Gd). The ^6P_J levels of Gd^{3+} ions are populated by an energy transfer (ET) process from $^8S_{7/2}$ (Gd)+($^3P_1$, $^3L_8$, $^3M_{10}$) (Ho)$\rightarrow{}^6P_J$ (Gd)+$^5I_8$ (Ho). A four-photon ET UC process was confirmed by the dependence of the $^6P_{7/2}$ level emission intensity on the pumping power. We found that the intensity of the UC emissions increased with Gd^{3+} ion concentration and peaked at 8 mol%, then starts to decrease until the Gd^{3+} ion concentration reached 70 mol%. The variation in the UV emission intensity is the result of the competition between the ET process and concentration quenching effect. Theoretical calculations based on steady-state equations validated the proposed UC mechanisms.

1. Introduction

Ultraviolet (UV) compact all-solid-state lasers have attracted much attention because of their potential applications in areas such as optical data storage, biomedical imaging, photodynamic therapy, environmental monitoring, and so on [1–3]. To produce UV lasers, continuous population of the corresponding high energy states is the key. Frequency upconversion (UC) by means of rare-earth ions' ladder-like energy levels is a promising technique to populate such high energy states, considering the availability of ample high-power infrared (IR) and visible diode lasers [4–7]. Recently, the UV UC emissions of Er^{3+}, Tm^{3+}, Pr^{3+}, Tb^{3+} and Ho^{3+} ions have been studied extensively [8–12]. Investigations on UV UC radiations of Gd^{3+} ions under IR pumping are still lacking till date due to the large energy gap (about 32,000 cm^{-1}) of Gd^{3+} ions [13–15].

Till now, only a handful papers reported the UC emissions of Gd^{3+} ions in the UV band. In 1994, Gharavi and Mcpherson [13] reported the UC emissions of Gd^{3+} in Er^{3+} doping $CsMgCl_3$ crystals under a 521.3 nm laser excitation. In 2008, Cao et al. [14] and Qin et al. [15] have obtained the UC emissions of Gd^{3+} in fluoride using Tm^{3+} and Yb^{3+} as sensitizers and a 980 nm laser diode (LD) as pump light. In 2009, Chen et al. [16] reported UC emissions of Gd^{3+} in Er^{3+} doped $NaYF_4$ under a 976 nm LD excitation. However, using Yb^{3+} and Ho^{3+} ions as co-sensitizers has never been tried before. In this letter, we report the observation of IR-to-UV UC emissions from Gd^{3+} ions in Yb^{3+}–Ho^{3+}–Gd^{3+} coexisting Y_2O_3 bulk ceramics under a 976 nm LD excitation. Both Yb^{3+} and Ho^{3+} ions served as sensitizers in the UC emissions of Gd^{3+} ions. Under the 976 nm LD excitation, Yb^{3+} ions absorbed the photons and continuously transferred energies to Ho^{3+} ions. Further energy transfer (ET) occurred from Ho^{3+} to Gd^{3+} and resulted in the UV UC emissions of Gd^{3+}.

2. Experimental

$Y_{1.838-x}Gd_xYb_{0.16}Ho_{0.002}O_3$ ($x=0$, 0.16, 0.4, 1, 1.4) nanocrystals were synthesized by the following route [17]:

Yttrium oxide (Y_2O_3, 99.99%), ytterbium oxide (Yb_2O_3, 99.99%), holmium oxide (H_2O_3, 99.95%) and gadolinium oxide (Gd_2O_3, 99.99%) were dissolved in nitric acid (all chemicals were purchased from Beijing Chemical Corporation and were used as received). After the solution was dried, the corresponding nitrates were obtained. The yttrium nitrate, ytterbium nitrate, holmium nitrate and gadolinium nitrate with corresponding mole ratio of cations were then completely dissolved in deionized water by stirring at a constant rate. Subsequently, citric acid was added into the solution with a 1:3 mole ratio of (Y+Gd+Ho+Yb) to citric acid. After complete dissolution, the pH of the solution was adjusted to 6.0 by addition of ammonium hydroxide. The resulting solution was dried at 120 °C for 24 h until it was transformed into a black bulk, which was further

* Corresponding authors.
E-mail addresses: zhangzhiguo@hit.edu.cn (Z. Zhang), cao@math.psu.edu (W. Cao).

0022-2313/$ - see front matter © 2010 Elsevier B.V. All rights reserved.
doi:10.1016/j.jlumin.2010.10.042

calcined at 800 °C for 2 h. The calcined powders were pressed into smooth and flat disks of 1 mm thick, which then were sintered at 1300 °C for 24 h to become ceramic. The X-ray diffraction pattern (XRD) of powder samples were recorded on Rigaku *D*/max-γB diffractometer using Cu $K\alpha$ radiation (λ=0.15418 nm). The UC emission spectra of the ceramic disks were measured under a power-tunable 976 nm laser diode (Hi-Tech Optoelectronics Co. Ltd., Beijing) excitation and detected by a lens-coupled monochromator with 3 nm spectral resolution (Zolix Instruments Co. Ltd., Beijing), which also has a photomultiplier tube (Hamamatsu CR131) attached. Luminescence lifetimes were measured using square-wave modulation of the electric current input to the 976 nm LD, and the signals were recorded via a Tektronix TDS 5052 digital oscilloscope. All experiments were performed at room temperature.

3. Results and discussion

Fig. 1 presents the XRD patterns of $Y_{1.838-x}Gd_xYb_{0.16}Ho_{0.002}O_3$ (x=0, 0.16, 0.4) samples and the standard XRD data for Y_2O_3 and Gd_2O_3. The diffraction peak positions correspond well to the standard powder diffraction pattern of Y_2O_3 (JCPDS 43-1036). The spectra indicated that all of the samples are in the cubic phase. The crystal structural symmetry of all samples is La3 (206), independent of the component ratios in starting materials.

Fig. 2 is a recording of the UC fluorescent radiation of the $Y_{1.678}Gd_{0.16}Yb_{0.16}Ho_{0.002}O_3$ bulk ceramic in the 300–440 nm wavelength range under a 976 nm LD excitation. Four emission bands have been generated by intra-4f electron transitions of Ho^{3+} and Gd^{3+} ions. The UC emissions centered at 309 and 315 nm are assigned to the $^6P_{5/2}\rightarrow{}^8S_{7/2}$ and $^6P_{7/2}\rightarrow{}^8S_{7/2}$ transitions of Gd^{3+}, respectively. Emissions that peaked at 392 and 428 nm originate from the $^3K_7/^5G_4\rightarrow{}^5I_8$ and $^5G_5\rightarrow{}^5I_8$ transitions of Ho^{3+}, respectively. The fourth emission band centered at 360 nm originates from the transition of ($^3P_1$, $^3L_8$, $^3M_{10}$)$\rightarrow{}^5I_7$ (Ho).

Although visible UC radiations of 520–800 nm have been widely discussed, they are also shown here in the inset of Fig. 2 to present a complete picture of the UC spectra. As illustrated in the inset, three UC emission bands centered at 540, 667 and 754 nm arise from $^5S_2/^5F_4\rightarrow{}^5I_8$, $^5F_5\rightarrow{}^5I_8$ (Ho) and $^5S_2/^5F_4\rightarrow{}^5I_7$ (Ho) transitions, respectively [18].

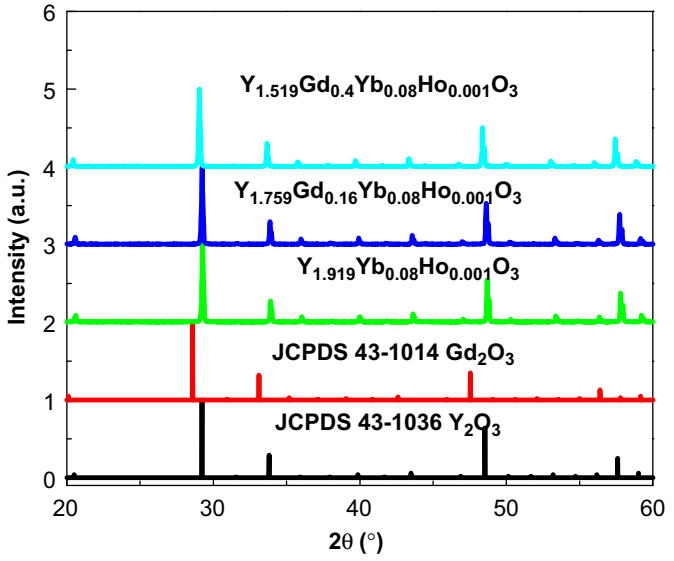

Fig. 1. Measured X-ray-diffraction spectrum of $Y_{1.838-x}Gd_xYb_{0.16}Ho_{0.002}O_3$ (x=0, 0.16, 0.4) bulk ceramics and the standard pattern of Y_2O_3 (JCPDS 43-1036) and Gd_2O_3 (JCPDS 43-1014).

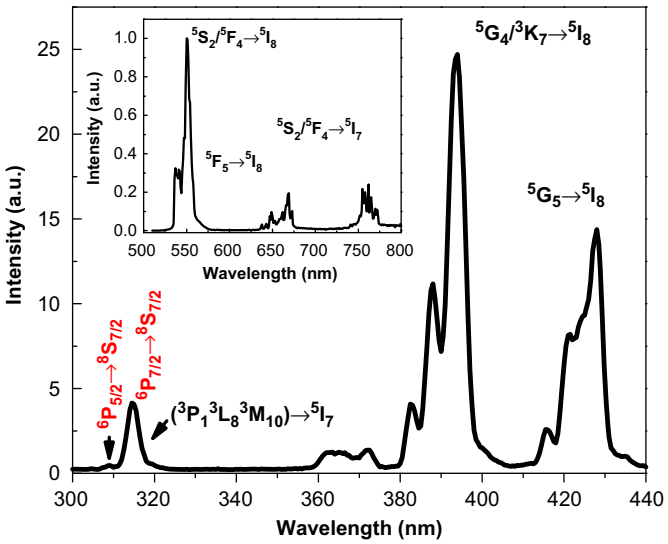

Fig. 2. UV and blue UC emission spectra of the $Y_{1.678}Gd_{0.16}Yb_{0.16}Ho_{0.002}O_3$ sample. The inset is the visible and NIR UC emission spectra of the $Y_{1.759}Gd_{0.16}Yb_{0.08}Ho_{0.001}O_3$ sample.

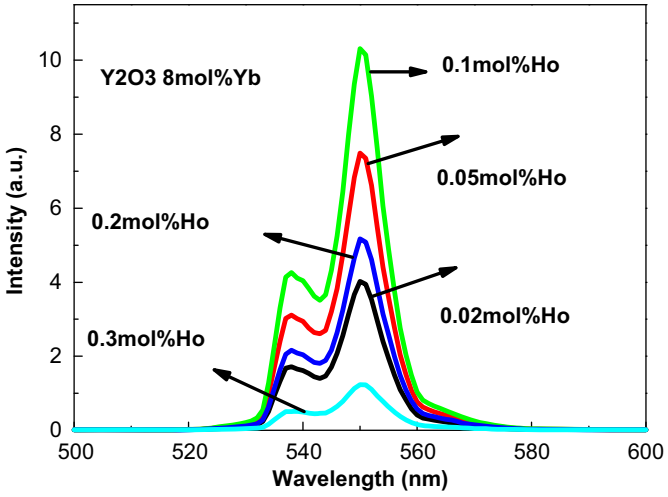

Fig. 3. Green UC emission spectra of the $Y_{1.84-x}Yb_{0.16}Ho_xO_3$ (x=0.0004, 0.001, 0.002, 0.004, 0.006) samples under 976 nm laser excitation.

Fig. 3 shows the green UC emissions in $Y_{1.84-x}Yb_{0.16}Ho_xO_3$ (x=0.0004, 0.001, 0.002, 0.004, 0.006) bulk ceramics under 976 nm LD excitation. As shown in Fig. 3, the fluorescence intensity increases steadily until the Ho^{3+} concentration reaches 0.1 mol%, beyond which the intensity decreases. Therefore, the Ho^{3+} ion concentration was chosen at 0.1 mol% in our investigation.

In the experiment, we found that the Gd purity was only "4 nines". In order to find if other rare-earth impurities could affect the UC emission spectra of $Y_{1.838-x}Gd_xYb_{0.16}Ho_{0.002}O_3$ (x=0, 0.16, 0.4, 1, 1.4) samples, in Fig. 4, we show the visible UC radiations of (a) 0.2 mol% Er^{3+}/8 mol% Yb^{3+}/Y_2O_3, (b) 0.2 mol% Tm^{3+}/8 mol% Yb^{3+}/Y_2O_3, (c) 0.1 mol% Ho^{3+}/8 mol% Yb^{3+}/Y_2O_3 under 976 nm LD excitation. As shown in Fig. 4, the characteristic spectra of Er^{3+} and Tm^{3+} ions were not observed in 0.1 mol% Ho^{3+}/8 mol% Yb^{3+}/Y_2O_3 bulk ceramic. Therefore, their amount, if non-zero, is too small to affect our experimental results.

Proposed UC processes are drawn in Fig. 5. In an Yb^{3+}–Ho^{3+}–Gd^{3+} coexisting system, Yb^{3+} ions successively transfer energy to Ho^{3+} to populate the $^5I_6$, $^5F_4/^5S_2$ and $^5G_{2,3}$ states. The electrons on $^5G_{2,3}$ states quickly and nonradiatively decay to the $^3K_7/^5G_4$ (Ho) and $^5G_5$ (Ho)

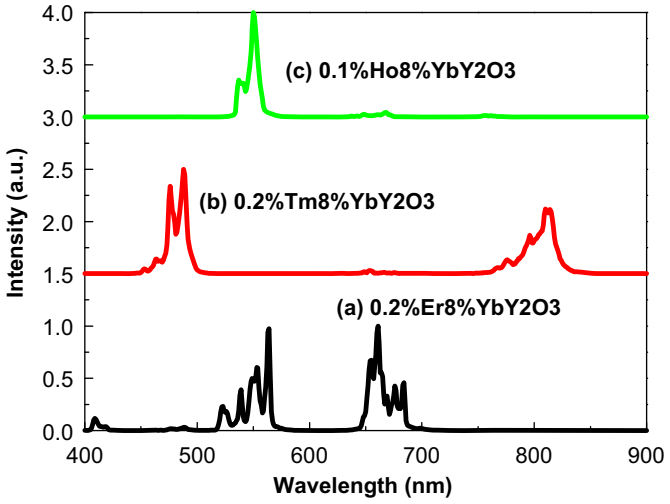

Fig. 4. UC emission spectra of (a) 0.2 mol% Er^{3+}/8 mol% Yb^{3+}/Y_2O_3, (b) 0.2 mol% Tm^{3+}/8 mol%Yb^{3+}/Y_2O_3, (c) 0.1 mol% Ho^{3+}/8 mol% Yb^{3+}/Y_2O_3 under 976 nm laser excitation.

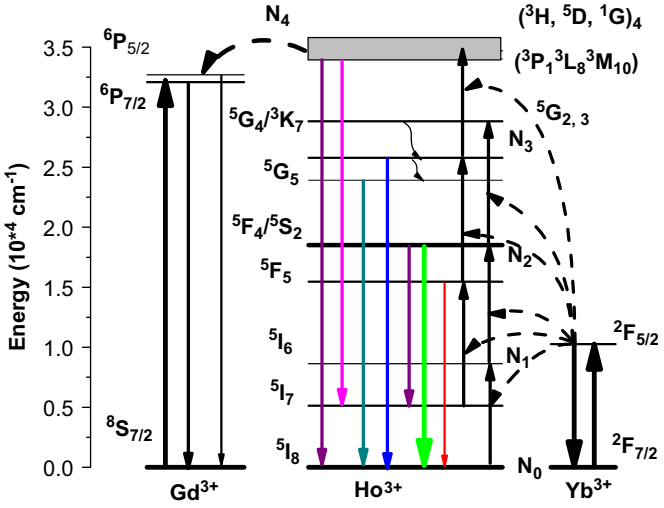

Fig. 5. Energy level diagrams of Gd^{3+}, Yb^{3+}, Ho^{3+} and upconversion emission processes.

states, which result in the 392 and 428 nm emissions, respectively. The energy transfer (ET) from Yb^{3+} ions in the $^2F_{5/2}$ state can also excite the Ho^{3+} ions from the $^5F_5$ state to the $^3K_7/^5G_4$ state. Further, Yb^{3+} ions successively transfer energy to Ho^{3+} to populate the (^3H, ^5D, $^1G)_4$ (Ho) states and then quickly and nonradiatively decay to the ($^3P_1$, $^3L_8$, $^3M_{10}$) (Ho) states. The transition of ($^3P_1$, $^3L_8$, $^3M_{10}$)→$^5I_7$ (Ho) leads to the emission centered at 360 nm. The Gd^{3+} ion cannot absorb 980 nm photons directly because of the large energy gap between the ground state and the first excited state. The possible mechanism considered in populating ^6P_J states of Gd^{3+} is the ET from ($^3P_1$, $^3L_8$, $^3M_{10}$) states of Ho^{3+}. Therefore, the transition of ^6P_J→$^8S_{7/2}$ leads to the UC emissions of Gd^{3+} peaked at 309 and 315 nm.

To better understand the UC processes, pump-power dependence of all intermediate emitting states involved is measured and displayed in Fig. 6. According to the relation $I_f \propto P^n$ [19], the n values for the green and red bands are about 2, consistent with the results reported before [20,21]. The n values obtained for 392 and 428 nm emissions are 3.1 and 3.0, respectively. This indicates that three-photon processes are needed to populate the $^3K_7/^5G_4$ and $^5G_5$ states. Additionally, it is noted that $n=2.2$ is obtained for populating the $^5S_2/^5F_4$ state, an additional one-photon process will lead to

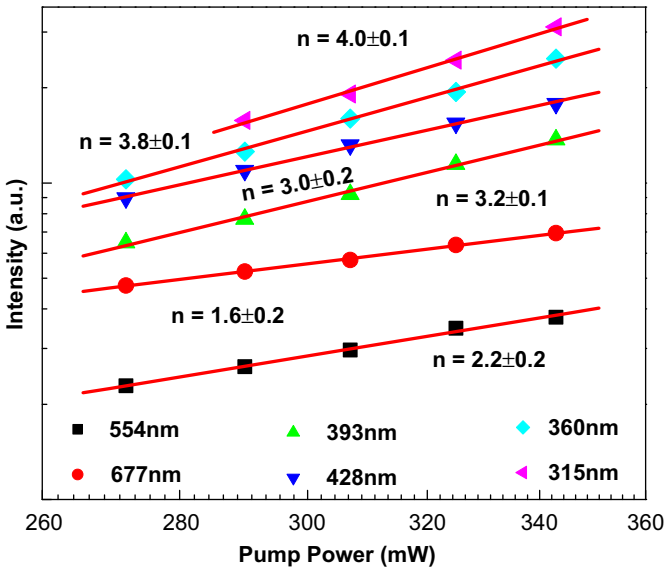

Fig. 6. The excitation power dependence of the emissions peaked at 315, 360, 393, 428, 554 and 667 nm in the $Y_{1.678}Gd_{0.16}Yb_{0.16}Ho_{0.002}O_3$ sample.

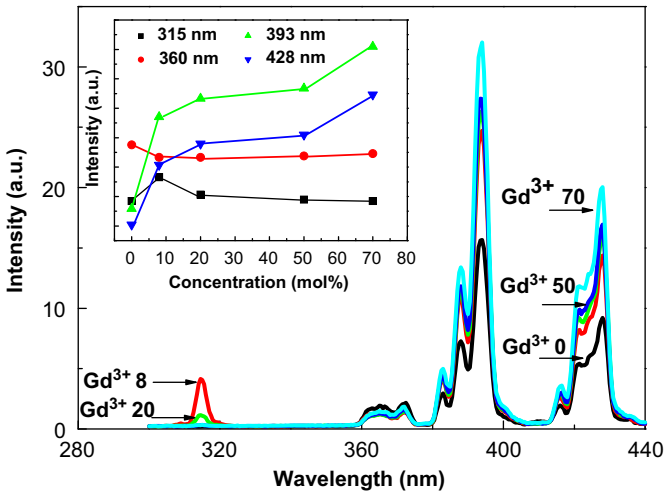

Fig. 7. UC emission spectra of the $Y_{1.838-x}Gd_xYb_{0.16}Ho_{0.002}O_3$ (x=0, 0.16, 0.4, 1, 1.4) samples under 976 nm laser excitation. The inset is the intensities of the 315, 360, 393 and 428 nm emissions as a function of Gd^{3+} ion concentration.

$n=3.2$ for populating the $^3K_7/^5G_4$ state, which agrees well with the observed value of $n=3.1$. Thus, the ET process from the $^5S_2/^5F_4$ state to the $^3K_7/^5G_4$ state by absorbing one-photon plays an important role to populate the $^3K_7/^5G_4$ state. For the emissions peaked at 360 and 315 nm, the n values are 3.8 ± 0.1 and 4.0 ± 0.1, respectively. The $n \approx 4$ indicates that populating the ($^3P_1$, $^3L_8$, $^3M_{10}$) (Ho) and ^6P_J (Gd) levels needs four 976 nm photons and therefore, involves the four-photon UC process. The n values of ($^3P_1$, $^3L_8$, $^3M_{10}$) and ^6P_J states, which are consistent with each other, give the evidence of ET from ($^3P_1$, $^3L_8$, $^3M_{10}$) to ^6P_J states.

In order to further understand the ET process and produce stronger UV UC emissions of Gd^{3+}, we optimized host materials by adjusting their components. Fig. 7 illustrates UC emission spectra of $Y_{1.838-x}Gd_xYb_{0.16}Ho_{0.002}O_3$ (x=0, 0.16, 0.4, 1, 1.4) samples in the 300–440 nm wavelength range, which are all recorded under the same conditions. The inset shows the intensity of the UC emissions centered at 315, 360, 392 and 428 nm as a function of the concentration of Gd^{3+}. We observed that the emission (315 nm)

intensity first increased then decreased with an increase in Gd^{3+} concentration, while the transition ($^3P_1$, $^3L_8$, $^3M_{10}$)→$^5I_7$ (Ho) first decreased then increased slightly. On the other hand, the intensity of the transitions $^3K_7/^5G_4$→$^5I_8$ and $^5G_5$→$^5I_8$ always increases with the concentration of Gd^{3+} ions. The variation in the fluorescence intensity in the spectra of Gd^{3+} implies that concentration quenching had occurred between Gd^{3+} ions when the doping is greater 8 mol%. Meanwhile, the reduced intensity of the transition ($^3P_1$, $^3L_8$, $^3M_{10}$)→$^5I_7$ creates more evidence of the ET from Ho^{3+} to Gd^{3+}. At the moment, we could not explain the increase in the transition ($^3P_1$, $^3L_8$, $^3M_{10}$)→$^5I_7$ and the UV UC emissions of Ho^{3+} with an increase in Gd^{3+} ion concentration.

Three transitions have occurred from ($^3P_1$, $^3L_8$, $^3M_{10}$) (Ho) to $^5I_8$ (Ho), $^5I_7$ (Ho) and $^5I_6$ (Ho) states, which lead to fluorescence radiations peaked at 306, 360 and 409 nm, respectively. [22]. However the ($^3P_1$, $^3L_8$, $^3M_{10}$)→$^5I_8$ transition (306 nm) could not be observed in our conditions. Only the ($^3P_1$, $^3L_8$, $^3M_{10}$)→$^5I_7$ (360 nm) and ($^3P_1$, $^3L_8$, $^3M_{10}$)→$^5I_6$ (409 nm) transitions have been observed, which are shown in Figs. 7 and 8, respectively. Their decay profiles are also obtained as shown in Fig. 9. Their decay profiles are in good agreement with each other. The variation in the intensity of the ($^3P_1$, $^3L_8$, $^3M_{10}$)→$^5I_6$ transition with the Gd^{3+} concentration provided an evidence for the ET from ($^3P_1$, $^3L_8$, $^3M_{10}$) to ^6P_J states. Therefore, we may compare the emission spectra from the $Y_{1.838}Yb_{0.16}Ho_{0.002}O_3$ and $Y_{1.678}Gd_{0.16}Yb_{0.16}Ho_{0.002}O_3$ samples in the range of 405–420 nm, as shown in Fig. 8. The spectra were all recorded under the same conditions (emission and excitation slits are 0.2 nm, high voltage of the photomultiplier tube is 900 V and the excitation power density is about 50 W/cm^2). For comparison, the emissions peaked at 409 and 415 nm are normalized to the 415 nm emission. From Fig. 8, the weak ($^3P_1$, $^3L_8$, $^3M_{10}$)→$^5I_6$ transition can be seen in the $Y_{1.838}Yb_{0.16}Ho_{0.002}O_3$ sample, which is marked by an asterisk (*), and this emission practically vanished in the $Y_{1.678}Gd_{0.16}Yb_{0.16}Ho_{0.002}O_3$ sample. The reduction in the emission intensity of the ($^3P_1$, $^3L_8$, $^3M_{10}$)→$^5I_6$ transition also offered another piece of evidence of the ET process.

To theoretically describe our proposed mechanism for the UV UC radiations, we use the following steady-state rate equations:

$$I\sigma_0 N_{Yb0}/h\nu - W_0N_0N_{Yb1} - W_1N_1N_{Yb1} - W_2N_2N_{Yb1} - W_3N_3N_{Yb1} - A_{Yb}N_{Yb1} = 0, \quad (1)$$

$$W_0N_0N_{Yb1} - W_1N_1N_{Yb1} - A_1N_1 = 0, \quad (2)$$

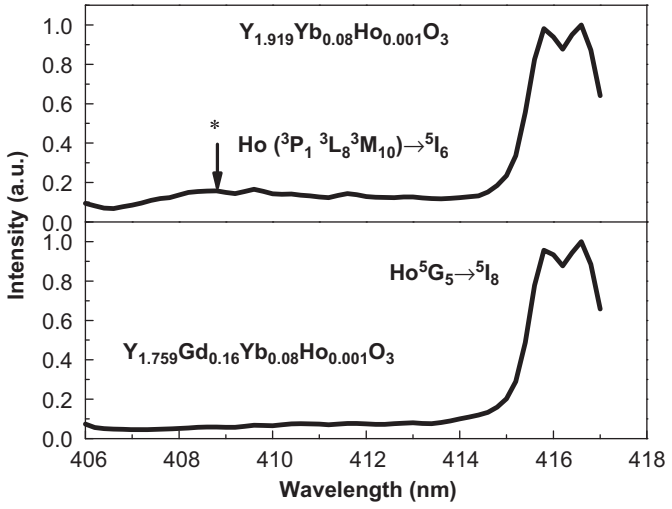

Fig. 8. UC emission spectra of $Y_{1.919}Yb_{0.08}Ho_{0.001}O_3$ and $Y_{1.678}Gd_{0.16}Yb_{0.16}Ho_{0.002}O_3$ in the 405–420 nm wavelength range recorded under the same conditions. The peaks marked by * is the transition from ($^3P_1$, $^3L_8$, $^3M_{10}$) (Ho) to $^5I_6$ (Ho) states.

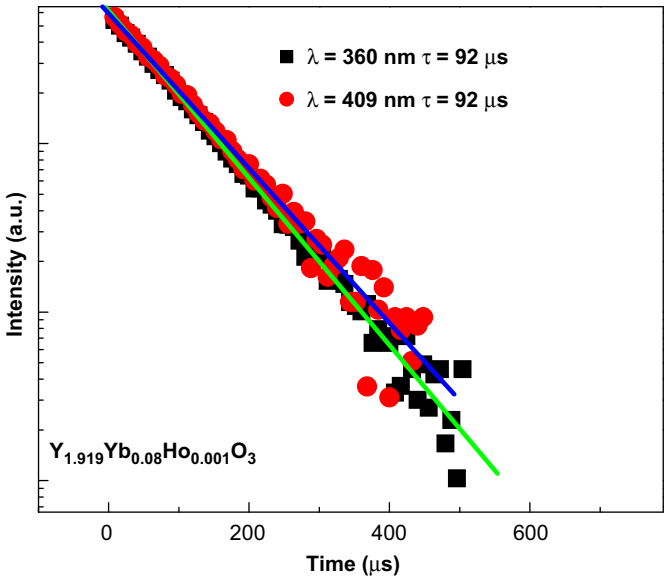

Fig. 9. Decay profiles of the ($^3P_1$, $^3L_8$, $^3M_{10}$)→$^5I_7$ (Ho) (360 nm) and ($^3P_1$, $^3L_8$, $^3M_{10}$)→$^5I_6$ (Ho) (409 nm) transitions in $Y_{1.838}Yb_{0.16}Ho_{0.002}O_3$ sample.

$$W_1N_1N_{Yb1} - W_2N_2N_{Yb1} - A_2N_2 = 0, \quad (3)$$

$$W_2N_2N_{Yb1} - W_3N_3N_{Yb1} - A_3N_3 = 0, \quad (4)$$

$$W_3N_3N_{Yb1} - CN_4N_{Gd0} - A_4N_4 = 0, \quad (5)$$

$$CN_4N_{Gd0} - A_{Gd}N_{Gd1} = 0, \quad (6)$$

where $N(W_i, A_i)$ $(i=0, 1, 2, 3, 4)$ are the population densities (energy transfer rates from excited Yb^{3+} ions, radiation rates) of the $^5I_8$, $^5I_6$, $^5S_2/^5F_4$, $^5G_4/^3K_7$ and ($^3P_1$, $^3L_8$, $^3M_{10}$) states of the Ho^{3+} ions; A_{Yb} and A_{Gd} are the radiation rates of the $^2F_{5/2}$ (Yb) and ^6P_J (Gd) states; N_{Yb0} and N_{Yb1} are the population densities of the Yb^{3+} ions in the ground and the excited states; N_{Gd0} and N_{Gd1} are the population densities of the Gd^{3+} ions in the ground and the excited states, ^6P_J, respectively; C is the energy transfer rate from excited Ho^{3+} ions to Gd^{3+} ions; I is the laser photon density; σ_0 denotes the absorption cross-section of the Yb^{3+} ions.

In our experiments, the radiation rates are much larger than the energy transfer rates. Thus, the energy transfer rates may be neglected so that the equations become:

$$N_{Yb1} = I\sigma_0 N_{Yb0}/(A_{Yb} + W_0N_0 + W_1N_1 + W_2N_2)h\nu \propto I, \quad (7)$$

$$N_3 = W_0W_1W_2N_0N_{Yb1}^3/A_1A_2A_3 \propto I^3, \quad (8)$$

$$N_4 = W_0W_1W_2W_3N_0N_{Yb1}^4/A_1A_2A_3A_4 \propto I^4, \quad (9)$$

$$N_{Gd1} = CW_0W_1W_2W_3N_{Gd0}N_0N_{Yb1}^4/A_1A_2A_3A_4A_{Gd} \propto I^4, \quad (10)$$

According to Eqs. (8)–(10), the $^5G_4/^3K_7$ (Ho) states should have a cubic dependence on the laser power while the (^3H, ^5D, $^1G)_4$/($^3P_1$, $^3L_8$, $^3M_{10}$) (Ho), ^6P_J (Gd) states have a biquadratic dependence on the laser power. These theoretical results agree well with experimental observations shown in Fig. 4.

4. Conclusion

In conclusion, $Y_{1.838-x}Gd_xYb_{0.16}Ho_{0.002}O_3$ $(x=0, 0.16, 0.4, 1, 1.4)$ bulk ceramic samples were synthesized through sintering the corresponding nanocrystal disks at 1300 °C. Under a 976 nm LD excitation, the oxide ceramics emitted UV UC fluorescence. The UV (309, 315 nm) UC emissions were assigned to the $^6P_{5/2}$, $^6P_{7/2}$→$^8S_{7/2}$

transitions of Gd^{3+} ions. Our experimental and theoretical data indicated that Ho^{3+} ions could transfer energy directly to Gd^{3+} ions by a four-photon UC process. At the moment, the origin of intensity enhancement of the UV (Ho) UC emissions with the Gd^{3+} ion concentration is not clear, which deserves future investigation.

Acknowledgment

This work was supported by the 863 Hi-Tech Researches and Development Programs of People's Republic of China.

References

[1] X. Zhang, C. Serrano, E. Daran, F. Lahoz, G. Lacostc, A. Muñoz-Yaüge, Phys. Rev. B 62 (2000) 4446.
[2] F. Xu, Z. Lü, Y.G. Zhang, G. Somesfalean, Z.G. Zhang, Appl. Phys. Lett. 88 (2006) 231109.
[3] F. Auzel, Chem. Rev. 104 (2004) 139.
[4] G.Y. Chen, G. Somesfalean, Z.G. Zhang, Q. Sun, F.P. Wang, Opt. Lett. 32 (2007) 87.
[5] H.J. Liang, G.Y. Chen, H.C. Liu, Z.G. Zhang, J. Lumin. 129 (2009) 197.
[6] R.K. Watts, J. Chem. Phys. 53 (1970) 3552.
[7] Livanova, et al., Opt. Spectrosc. 24 (1968) 340.
[8] Z. Pan, A. Ueda, R. Mu, S.H. Morgan, J. Lumin. 126 (2007) 251.
[9] X.Y. Wang, H. Lin, D.L. Yang, J. Appl. Phys. 101 (2007) 113535.
[10] M. Malinowski, M. Kaczkan, S. Stopiński, R. Piramidowicz, A. Majchrowski, J. Lumin. 129 (2009) 1505.
[11] C.H. Hu, C.L. Sun, J.F. Li, Z.S. Li, H.Z. Zhang, Z.K. Jiang, Chem. Phys. 325 (2006) 563.
[12] L.H. Huang, T. Yamashita, R. Jose, Y. Arai, T. Suzuki, Y. Ohishi, Appl. Phys. Lett. 90 (2007) 13116.
[13] A.R. Gharavi, G.L. Mcpherson, J. Opt. Soc. Am. B 11 (1994) 913.
[14] C.Y. Cao, W.P. Qin, J.S. Zhang, Y. Wang, P.F. Zhu, G.D. Wei, G.F. Wang, R.J. Kin, L.L. Wang, Opt. Lett. 33 (2008) 857.
[15] W.P. Qin, C.Y. Cao, L.L. Wang, J.S. Zhang, D.S. Zhang, K.Z. Zheng, Y. Wang, G.D. Wei, G.F. Wang, P.F. Zhu, R.J. Kim, Opt. Lett. 33 (2008) 2167.
[16] G.Y. Chen, H.J. Liang, H.C. Liu, G. Somesfalean, Z.G. Zhang, Opt. Express 17 (2009) 16366.
[17] G.Y. Chen, Y. Liu, Z.G. Zhang, B. Aghahadi, G. Somesfalean, Q. Sun, F.P. Wang, Chem. Phys. Lett. 448 (2007) 127.
[18] X.X. Luo, W.H. Cao, Mater. Lett. 61 (2007) 3696.
[19] M. Pollnau, D.R. Gamelin, S.R. Lüthi, H.U. Güdel, M.P. Hehlen, Phys. Rev. B 61 (2000) 3337.
[20] Y. Yu, Y.D. Zheng, F. Qin, Z.M. Cheng, C.B. Zheng, Z.G. Zhang, W.W. Cao, J. Lumin., in press, doi:10.1016/j.jlumin.2010.09.033.
[21] X. Yang, S. Xiao, Z. Liu, X.H. Yan, Appl. Phys. B. 86 (2007) 77.
[22] M. Kowalska, G. Klocek, R. Piramidowicz, M. Malinowski, J. Alloys Compd. 380 (2004) 156.